Competition between cotunneling, Kondo effect, and direct tunneling in discontinuous high-anisotropy magnetic tunnel junctions

D. Ciudad,[1,2,*] Z.-C. Wen,[3,†] A. T. Hindmarch,[1,‡] E. Negusse,[4] D. A. Arena,[4] X.-F. Han,[3] and C. H. Marrows[1,§]

[1]*School of Physics and Astronomy, University of Leeds, Leeds LS2 9JT, United Kingdom*

[2]*Francis Bitter Magnet Laboratory, Massachusetts Institute of Technology, Cambridge, Massachusetts 02139, USA*

[3]*Beijing National Laboratory of Condensed Matter Physics, Institute of Physics, Chinese Academy of Sciences, Beijing 100190, China*

[4]*National Synchrotron Light Source, Brookhaven National Laboratory, Upton, New York 11973, USA*

(Received 5 September 2011; revised manuscript received 5 May 2012; published 7 June 2012)

The transition between Kondo and Coulomb blockade effects in discontinuous double magnetic tunnel junctions is explored as a function of the size of the CoPt magnetic clusters embedded between AlO_x tunnel barriers. A gradual competition between cotunneling enhancement of the tunneling magnetoresistance (TMR) and the TMR suppression due to the Kondo effect has been found in these junctions, with both effects having been found to coexist even in the same sample. It is possible to tune between these two states with temperature (at a temperature far below the cluster blocking temperature). In addition, when further decreasing the size of the CoPt clusters, another gradual transition between the Kondo effect and direct tunneling between the electrodes takes place. This second transition shows that the spin-flip processes found in junctions with impurities in the barrier are in fact due to the Kondo effect. A simple theoretical model able to account for these experimental results is proposed.

DOI: 10.1103/PhysRevB.85.214408 PACS number(s): 72.25.−b, 75.76.+j, 73.23.Hk, 72.15.Qm

I. INTRODUCTION

Conventional spintronic devices make use of currents comprising a large number of spin-polarized carriers,[1] in which the quantum properties of the electron are averaged away. The development of single-electron spintronic devices addresses this issue.[2,3] The Coulomb blockade (CB) effect reveals the quantization of charge, while phenomena such as the Kondo effect rely on the quantum nature of spin. One experimental approach has been the use of double magnetic tunnel junctions (DMTJs) with metallic clusters between two barriers. Electrically isolated conductive clusters have a charging energy E_c. Transport is suppressed (CB effect) when the applied bias $eV \lesssim E_c$ and the thermal energy $k_BT \lesssim E_c$. In DMTJs, the interplay between spin-dependent tunneling processes and CB gives rise to experimentally observed phenomena such as spin accumulation,[4] cotunneling enhancement of the tunnel magnetoresistance (TMR),[5–7] TMR oscillation with bias,[8] enhanced spin lifetimes,[9] Kondo physics,[10] the generation of electromotive forces,[11] and anisotropic magneto-Coulomb effects.[12]

The suppression of conductance by the CB is not perfect, however. It is still possible that cotunneling of two electrons in and out of the cluster can take place simultaneously.[13] An enhancement of the TMR can then take place due to this coherence.[14] However, some limitations arise through Kondo-like physics when using magnetic clusters.[15] While a cotunneling conduction regime can give rise to an enhancement of the TMR, the Kondo effect can suppress TMR by enhancing the antiparallel conductance of the junction.[3] The coexistence of Kondo and ferromagnetic phases in DMTJs has clearly been shown recently.[16] The transition from Kondo to cotunneling has been supposed to be correlated with the suppression of the fluctuations of the magnetic moment in the clusters.[10] Studying the transition between both regimes is important to determine the limitations of future single-electron spintronic devices on the one hand, and to clarify the physical foundations of the coexistence of ferromagnetism and the Kondo effect on the other.

Here we use DMTJs with CoPt nanoclusters embedded within the barrier to show the existence of a competition between cotunneling and Kondo effects on TMR, instead of the sharp crossover as previously reported in Ref. 10. Due to the enhanced magnetic anisotropy in CoPt, the coexistence of both effects has been found even in the same sample, with a gradual transition between the two as a function of the temperature. As the transition occurs far below the blocking temperature, this clearly points out that the transition between Kondo and cotunneling is not directly related to the suppression of the fluctuations of the magnetic moments, as previously thought.[10] When further reducing the size of the clusters, a gradual transition between the Kondo effect and direct tunneling between the magnetic electrodes is found.

II. EXPERIMENTAL RESULTS

A. Growth and characterization of the $Co_{75}Pt_{25}$ nanoclusters

Three different types of structure have been grown by sputtering onto thermally oxidized Si wafer substrates: one to determine the shape of the clusters by scanning tunneling microscopy (STM), another to characterize the magnetism and oxidation state of the clusters by superconducting quantum interference device (SQUID) magnetometry and soft-x-ray absorption spectroscopy (SXAS) and magnetic circular dichroism (SXMCD), and the third structure is the DMTJs themselves. The clusters of CoPt were obtained by depositing nominal layer thicknesses <2 nm onto the first of two amorphous alumina (AlO_x) tunnel barriers. Due to the surface energy mismatch, CoPt aggregates into nanoscale clusters. For each structure, a set of different thicknesses (t) of $Co_{75}Pt_{25}$ was deposited. First, by using a shadow shutter, a $Co_{75}Pt_{25}$ layer was grown in a wedge shape whose thickness spans $t = 0$–1.1 nm across the sample. Additionally, another four different samples were grown as references, with t being 0,

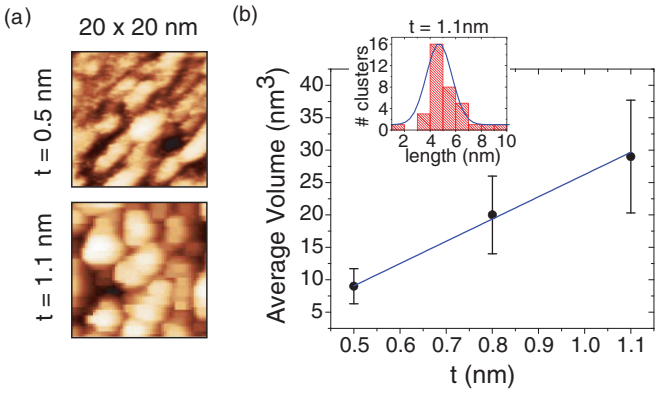

FIG. 1. (Color online) (a) STM images of the CoPt nanoclusters for different nominal layer thicknesses t. (b) Average cluster volume estimated by fitting the histogram of the cluster sizes to a log-normal distribution, as shown in the inset.

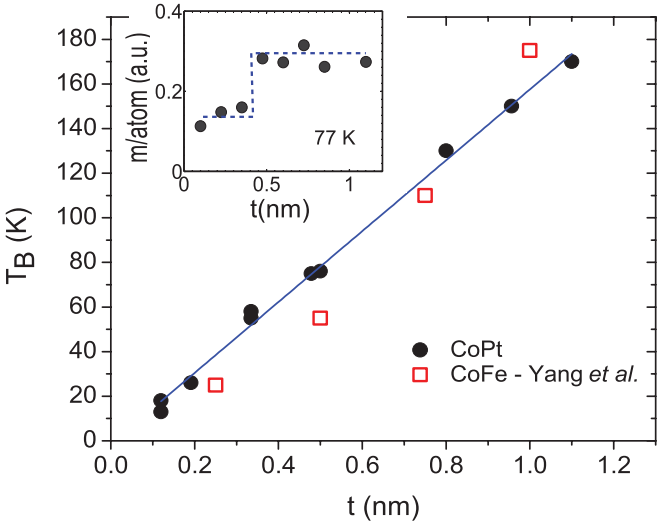

FIG. 2. (Color online) Blocking temperature T_B (determined from SQUID FC and ZFC measurements) vs nominal layer thickness t of CoPt and CoFe (CoFe data from Ref. 10 by Yang *et al.*). The inset shows the magnetic moment per atom—from SXMCD—vs t. The dotted line is a guide to the eye.

0.5, 0.8, and 1.1 nm. The deposition was done by rf-assisted sputtering in an Ar atmosphere of 0.6 mTorr, with a base pressure of 2.0×10^{-8} Torr, and with a 100 Oe magnetic field applied in the sample plane. AlO_x barriers were obtained by glow-discharge oxidizing an Al layer as described in Ref. 17.

For STM measurements, the structure was $Ru(10)/AlO_x(1)/Co_{75}Pt_{25}(t)$, with thicknesses in nm. STM measurements allow us to estimate the volume of the clusters. As found in previous work,[10,18] the clusters have a "pancake" form. In our samples, these "pancakes" have an elongated shape that tends to become more rounded when increasing t, as shown in Fig. 1(a). Cluster volumes V were estimated in a naive way by directly multiplying the average length, width, and height. These parameters were determined by fitting log-normal distributions to the histograms of the clusters sizes, as shown in the inset of Fig. 1(b). The change of the average volume $\langle V \rangle$ of the clusters varies with t, as shown in Fig. 1(b). A least-squares linear fit (LSL) of these data gives a correlation coefficient $R^2 = 0.995$. Similar sizes have been reported for Co grown onto AlO_x, where a linear relationship between $\langle V \rangle$ and t was also found.[19]

For SXAS and SXMCD measurements, the structure grown was $Ru(10)/AlO_x(1)/Co_{75}Pt_{25}(t)/AlO_x(1)/Ta(1)$. These samples were grown at the same time as those for STM measurements, using a shadow shutter to avoid the last two layers for the STM set. The measurements were carried out at the U4B beamline[20] using methods described in previous work.[21,22] For SXAS the beamline was set up to provide linearly polarized light with an energy resolution ~0.5 eV at the Co L_3 edge (~778 eV). For SXMCD measurements, the beam was 90% circularly polarized with a resolution of ~1 eV at that energy. Data were collected in total electron yield mode and normalized to the incident beam intensity using a Au grid monitor. The x-ray beam was swept along the wedge in t (from $t = 0$ to 1.1 nm over a distance ~23 mm), measuring both XAS and XMCD at different positions. The beam was shaped to reduce as much as possible the spread in t in each measurement (~2 mm in the wedge direction). The data taken from the samples with fixed CoPt thickness and those slices of the wedge with the same average CoPt thickness correspond very closely. No oxidation features such as those previously reported[22] where found in the Co SXAS spectra (data not shown). The average magnetic moment per Co atom at 77 K, determined from SXMCD, is given in the inset of Fig. 2, which appears to collapse when $t \lesssim 0.4$ nm.

Subsequently, the wedge was diced into ~2 mm broad slices along the wedge direction for SQUID magnetometry. For each slice, and for the samples with fixed CoPt thickness, field-cooled (FC) and zero-field-cooled (ZFC) measurements were performed according to the protocol prescribed by Hansen and Mørup.[23] Prior to measurement, the sample was cooled from room temperature to 1.5 K in zero field. The ZFC measurements were then acquired while warming the sample in a field of 50 Oe. The sample was then cooled again in this 50 Oe field while the FC measurements were taken. The blocking temperature T_B was determined from the maximum value of the magnetic moment in the ZFC curve just before it joins the FC curve, corresponding to T_B for the largest clusters in the sample. Figure 2 shows that $T_B \propto t$ (LSL also gives $R^2 = 0.995$). The SQUID data explain the drop in magnetic moment below $t \sim 0.4$ nm in the SXMCD data: it is associated with the transition to the superparamagnetic state as T_B becomes smaller than the 77 K liquid nitrogen SXMCD measurement temperature.

Taking the $t = 1.1$ nm clusters as an example, which have a volume $\langle V \rangle$ of 29 nm^3 and $T_B \approx 180$ K, we apply the classical relation $K \approx 25 k_B T_B / \langle V \rangle = 1600$ kJ/m^3 to obtain the magnetic anisotropy of the clusters K. The 25 factor is related to the time scale of the measurement being appropriate for SQUID, SXMCD, and transport data. This will be an overestimate as our T_B will correspond to clusters larger than $\langle V \rangle$, but gives a useful estimate that lies within the broad span of values of the magnetic anisotropy of CoPt that can be found in the literature. As expected, it is somewhat less than for the equiatomic $L1_0$-ordered phase,[24] where $K \sim 4900$ kJ/m^3.

We also compare our $T_B(t)$ data to those for CoFe clusters obtained by Yang *et al.* in Fig. 2.[10] Some important differences

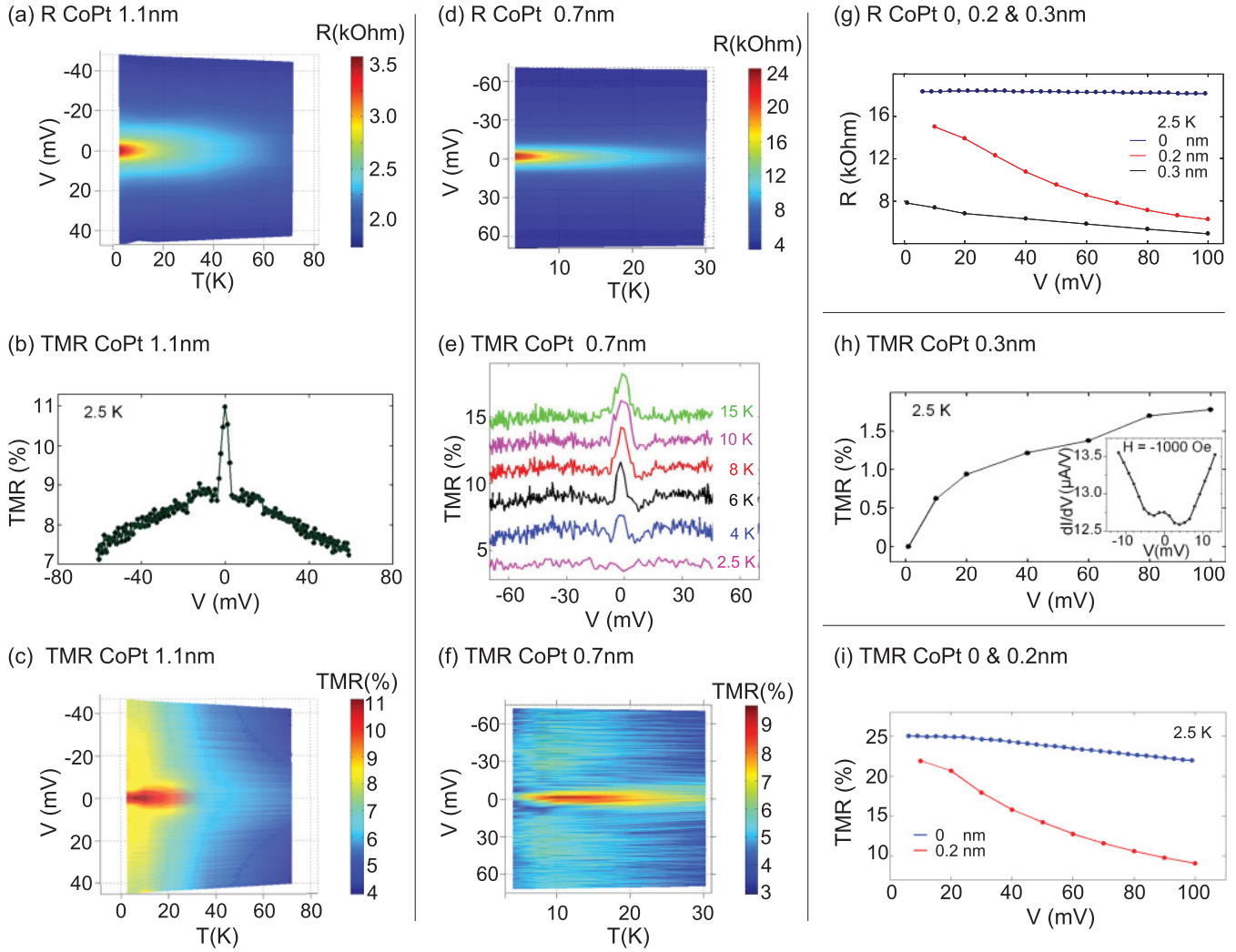

FIG. 3. (Color online) Magnetotransport data: resistance R at a saturating magnetic field of 8 T and TMR of DMTJs against V and T for different nominal CoPt thicknesses t. For $t = 1.1$ nm there is an enhancement of R (a) and TMR [(b) and c)] due to co-tunneling; for $t = 0.7$ nm, R is also enhanced (d) and we see TMR enhancement or suppression depending on T [(e) and (f)]. Offsets have been added for clarity in (e). Resistances at 2.5 K for $t = 0$, 0.2 and 0.3 nm are shown in (g). For $t = 0.3$ nm, (h) a strong Kondo TMR suppression is observed at $T = 2.5$ K (dynamic conductance measurements are shown in the inset); for $t = 0$ and 0.2 nm (i) we observe a TMR reduction due to spin scattering at 2.5 K.

can be found between both alloys. T_B in CoPt clusters is closely proportional to t, whereas there is some weak curvature to the CoFe data. The linear relationship between $\langle V \rangle$ and t (Fig. 1) is close to a proportionality, indicating that all the clusters, no matter what their size, have roughly the same anisotropy, suggesting surface anisotropy effects are comparatively weak compared to bulk ones.

B. Magnetotransport measurements

The complete structure of our DMTJs was Ta(5)/ Ru(20)/ Ta(5)/$Ni_{80}Fe_{20}$(3)/$Ir_{22}Mn_{78}$(12)/$Co_{25}Fe_{75}$(4)/ Ru(0.8)/$Co_{25}Fe_{75}$(4)/AlO_x(1)/$Co_{75}Pt_{25}$(t)/AlO_x(1)/$Co_{25}Fe_{75}$(4)/Ru(0.8)/$Co_{25}Fe_{75}$(4)/$Ir_{22}Mn_{78}$(12)/Ta(5)/Ru(6), comprising two CoFe outer electrodes with a layer of CoPt nanoclusters in between two alumina barriers. Both CoFe electrodes are pinned, with each part of a synthetic antiferromagnet, designed to reduce any effect of stray fields. DMTJ mesas were defined by photolithography and plasma etching,[17] of area 120 μm $\times$ 40 μm. Magnetotransport measurements were performed using a standard four-probe ac measurement technique in a gas-flow He cryostat able to achieve an 8 T magnetic field. In order to check the quality of our barriers, the low T current-voltage I-V characteristic of junctions without any CoPt layer ($t = 0$) was fitted to Simmons' model[25] by a least-squares method. Simmons' intermediate voltage equations match our data excellently for a barrier thickness of 1.9 nm and a height of 1.8 eV, very reasonable values for a nominally 2-nm-thick AlO_x barrier.

Meanwhile, DMTJs with a $t = 1.1$ nm CoPt layer showed CB features typical of those previously found in similar structures.[5,6,10,18,26] The main fingerprint of the CB effect is a strong enhancement of the dependence of the conductance with bias V at low T, as shown in Fig. 3(a). In addition, we also observed an increase of the TMR at low bias ($V \lesssim 5$ mV) and temperature ($T \lesssim 30$ K), as shown in Figs. 3(b) and 3(c),

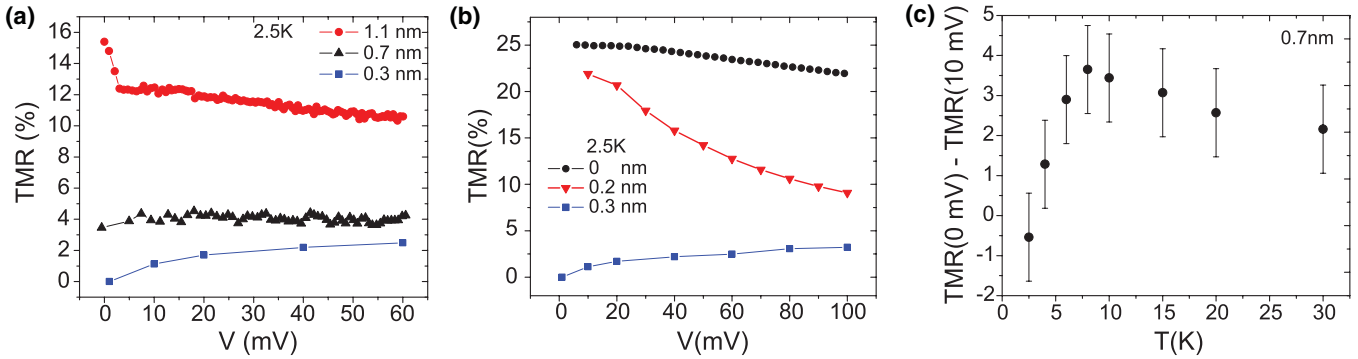

FIG. 4. (Color online) Magnetoresistance measurements. (a) TMR of DMTJs vs V for $t = 1.1$, 0.7, and 0.3 nm at 2.5 K. When reducing the CoPt thickness, the TMR varies from being enhanced to being suppressed at low V. (b) TMR vs V for $t = 0.3$, 0.2, and 0 nm at 2.5 K. With thicknesses below $t = 0.3$ nm, the TMR is recovered. (c) The amplitude of the TMR at low bias, defined as the difference on the TMR when applying 0 and 10 mV, respectively, as a function of T for $t = 0.7$ nm. Two different regimes are clearly identified.

which is consistent with the DMTJ entering the cotunneling transport regime.[5,6,10] We define TMR as the fractional change in resistance between -0.1 and 8 T.

If the thickness of the CoPt layer is reduced to $t = 0.7$ nm, we still find the enhancement of the resistance R and TMR at similarly low bias and temperature, as shown in Figs. 3(d)–3(f). However, a novel effect is observed: when T is lowered below about 8 K, the low bias cotunneling peak in the TMR starts to drop and is completely suppressed at 2.5 K. Clearly another effect is competing with the cotunneling enhancement to reduce the TMR, something that the Kondo effect is known to do.[10,15] The Kondo effect flips the spins of the electrons passing through the clusters, effectively reducing the polarization of this current and thus reducing the TMR.

When t is reduced further, to 0.3 nm, the enhancement of the resistance at low bias and temperature disappears, as shown in Fig. 3(g). Figure 3(h) shows that the TMR is suppressed to zero at low bias ($V \lesssim 20$ mV), further evidence for the Kondo effect. Furthermore, when the dynamic conductance dI/dV of this sample is measured at helium temperature [inset to Fig. 3(h)], a weak asymmetric peak is seen at low bias, at a field of -1000 Oe after the application of $+3000$ Oe. The peak was not present in a prior measurement at zero field. Such a peak is associated with a Kondo resonance on the nanoclusters[27] and can only survive when the outer electrodes are antiparallel,[15] as here. It is comparable in amplitude to that seen by Yang *et al.*,[10,28] but rather narrower: its width ΔV of a few mV implies a lower Kondo temperature $T_K = e\Delta V/k_B \approx 20$ K.[27] The appearance of the Kondo resonance is only expected in the presence of large magnetic moments in the clusters if there is a high magnetic anisotropy,[29,30] as we have here in our CoPt dots.

Interestingly, if the CoPt layer thickness is further reduced, the resistance —Fig. 3(g)— and TMR are recovered. Figure 3(i) shows the TMR for a DMTJ with $t = 0.2$ nm and for a tunnel junction without CoPt clusters ($t = 0$ nm). This is consistent with some previous experiments dealing with impurities in the barrier.[31,32] It is noteworthy that the spin-flip process is observed for CoPt clusters that still are thermally stable ferromagnets (see Fig. 2). The experimental data imply that the tunnel conductance in DMTJs with clusters within this range of sizes can be understood as the addition of two competing terms: direct tunneling and tunneling through the clusters showing the Kondo effect.

In order to clearly show how the discussed transitions gradually compete as a function of the size of the clusters, Figs. 4(a) and 4(b) show the TMR versus bias just at 2.5 K for the different junctions. In Fig. 4(a), it can be seen how the TMR is reduced when reducing the nominal thickness of the CoPt layer from 1.1 to 0.3 nm. Previously, we have discussed how the low TMR peak at low bias for the junctions with $t = 0.7$ nm evolves with temperature showing the transition from cotunneling enhancement to Kondo suppression of the TMR. This figure also helps to clarify why for $t = 0.7$ nm the TMR does not increase with increasing bias voltage as the junctions with $t = 0.3$ nm do. Even at 2.5 K, where the low temperature and bias peak have disappeared, the $t = 0.7$ nm junctions are showing a mixed behavior between Kondo and cotunneling. Figure 4(b) shows how the TMR is recovered when the nominal thickness is reduced below $t = 0.3$ nm.

The transition between Kondo and cotunneling with T in the $t = 0.7$ nm junctions is also clearly shown in Fig. 4(c). In this figure, the change of the amplitude of the TMR peak defined as $\mathrm{TMR}(V = 0) - \mathrm{TMR}(V = 10\ \mathrm{mV})$ is plotted versus temperature. Two different behaviors are clearly found that gradually compete.

III. THEORETICAL MODEL

A. Conductivity

The experimental data suggest that the tunnel conductivity σ in the CoPt junctions can be understood as the addition of three main terms:

$$\sigma = a\sigma_D + b(\sigma_E + \sigma_K), \tag{1}$$

with $a + b = 1$. Here, σ_D is the direct tunneling conductivity between the outer electrodes, σ_E is the elastic conductivity through the clusters without spin flips, and σ_K is the conductivity through the clusters showing the Kondo effect. The contribution of each term depends on the fractional populations of clusters, which is taken into account through the parameters a and b, and on the voltage and the temperature through σ_D,

σ_E, and σ_K. For very thin layers, $a > b$ since there are few clusters within the barrier and most of the electrons must directly tunnel. When the thickness of the intermediate CoPt layer is increased, b must also increase while a decreases since there are more opened channels within the barrier due to the higher number of clusters.

In the CoPt junctions studied here, for $t \to 0$ nm, $a\sigma_D$ dominates; for $t \sim 3$ nm and $T = 2$ K, $b\sigma_K$ does. For thicker CoPt layers, $b\sigma_E$ rapidly increases. The TMR depends on which is the main contribution to σ. For example, if σ_K is the main term, the Kondo effect dominates the overall behavior and the TMR is reduced. On the other hand, if σ_E is predominant, the TMR is enhanced at low temperature due to cotunneling. For higher temperature, σ_E will still be dominating, and so there is no enhancement of the TMR since the elastic tunneling is in the sequential regime (without CB effects). The transitions are gradual and depend on the temperature and the size of the clusters.

The model is similar to those previously suggested for explaining the TMR behavior in junctions with impurities in the barrier.[31–33] Jansen and Moodera consider three different conduction paths: direct, through nonmagnetic impurities, and through magnetic impurities.[31,33] In particular, the conductance with spin-exchange scattering is taken from the Appelbaum[34,35] and Anderson[36] models, a perturbation theory of the conductance originally developed to explain the zero bias anomalies in DMTJs due to the contribution to the tunneling current of localized states within the barrier, which is also called the Kondo effect.[6,34–36] Remarkably, the spin-flip process is found in CoPt discontinuous layers that still are thermally stable ferromagnets, which suggests that the spin-flip processes found in dusted DMTJs are in fact Kondo-based.

We will now evaluate the different conductivity terms in Eq. (1) in order to study the gradual transition between cotunneling enhancement and Kondo suppression of the TMR. Our aim here is not to provide a quantitative fit to the data, but rather to put forward a simplified picture that captures the essential physics of the situation. In particular, we will check if the simple theoretical model suggested can explain the coexistence of cotunneling and the Kondo effect in the same junction, with the gradual transition between both effects tuned by T, as we have experimentally found for the CoPt junctions with $t = 0.7$ nm. Let us assume for simplicity that there is no dispersion of the distribution of the size of the clusters. We must remark that the dispersion of the size of the CoPt clusters we experimentally find [see the inset in Fig. 1(b)] is similar to the dispersion of the sizes found by Yang *et al.*[10] but the transitions found in our work are gradual instead of sharp crossovers.

For σ_D, the classical formula given by Simmons could be considered.[25] However, for studying this transition, we will consider that the direct tunneling is negligible: $a = 0$ and $b = 1$. In that case: $\sigma = \sigma_E + \sigma_K$.

According to Goldhaber-Gordon *et al.*,[37] for a broad range of temperatures and in particular for temperatures close to T_K,

$$\sigma_K = \sigma_0 \left(\frac{T_{K2}^2}{T^2 + T_{K2}^2} \right)^S, \tag{2}$$

where

$$T_{K2} = \frac{T_K}{\sqrt{2^{1/S} - 1}}. \tag{3}$$

In the Kondo regime, $S \approx 0.2$. The parameter σ_0 varies with the cluster occupancy. For symmetric barriers, $\sigma_0 \leqslant (2e^2)/h$, where e is the charge of the electron and h is Planck's constant. In the case of the junction with $t = 0.3$ nm, we have experimentally found $T_K \approx 20$ K. For the junctions with $t = 0.7$ nm, we assume a Kondo temperature of the same order: $T_K \approx 10$ K.

Following Takahashi and Maekawa,[14] in the cotunneling regime ($k_B T \ll E_c$), $\sigma_E = \sigma_{\text{cot}}$, where

$$\sigma_{\text{cot}} = \frac{2h}{3e^2} \frac{1}{R_T^2} \left(\frac{k_B T}{E_c} \right)^2, \tag{4}$$

where R_T is the tunnel resistance between one electrode and the clusters and E_c is the charging energy. In the high-temperature limit ($k_B T \gg E_c$), the sequential tunneling dominates and $\sigma_E = \sigma_{\text{seq}}$, where

$$\sigma_{\text{seq}} = (2R_T)^{-1} \left(1 + \frac{E_c}{3k_B T} \right)^{-1}. \tag{5}$$

Considering a gradual change from sequential tunneling to cotunneling, we can write for any temperature

$$\sigma_E = \sigma_{\text{cot}} + \sigma_{\text{seq}}. \tag{6}$$

We can evaluate R_T by using Eq. (5). At very high temperature, $\sigma \approx \sigma_{\text{seq}} = (2R_T)^{-1}$. In this limit, the resistance of the 0.7 nm CoPt junctions is $\approx$8 kΩ: Figure 3(b) gives its evolution below 30 K. Thus, for these junctions, $R_T \approx 4$ kΩ.

Next, we write $E_c = e^2/(2C)$, where C the capacitance of the clusters, which depends on their shape. To simplify, we will model the clusters as isolated spheres having the volume that we have experimentally determined. In that case, C is given by $C = 4\pi\epsilon\epsilon_0 r_{\text{eff}} = 4\pi\epsilon\epsilon_0 \sqrt[3]{\frac{3}{4}\frac{V}{\pi}}$. Here ϵ_0 is the vacuum permittivity, ϵ is the relative permittivity of the insulating barrier, r_{eff} is the effective radius of the sphere, and V is the volume of the clusters. For Al_2O_3, $\epsilon = 8$.[38] As shown in Fig. 1(b), the volume for the $t = 0.7$ nm CoPt clusters is $V \approx 15$ nm^3. These values give a capacitance for the $t = 0.7$ nm junctions of $C \approx 1.4$ aF. The effect of the electrodes on the capacitance could also be considered, but this is just a small correction.[38]

These equations show that the transition from Kondo to cotunneling can be gradual *even for no dispersion in cluster size*, as we found in the CoPt junctions with $t = 0.7$ nm. The value of σ_0 depends on the site occupancy n_d. Both n_d and T_K are functions of the temperature—which produces a broadening of the energy levels—and also of the difference of energies between the Fermi energy of the leads and the first localized level in the cluster below, which is a function of the size of the clusters. Thus, σ_0 is correlated with the Kondo temperature T_K through this size dependence: the higher T_K, the smaller the value of σ_0.[37] Obviously if $\sigma_0 = 0$, then $\sigma = \sigma_E$. On the other hand, if it takes its maximum possible value, $\sigma_0 = (2e^2)/h$, we find $\sigma \approx \sigma_0$ since $\sigma_0 \gg \sigma_E$ for any temperature in between 2 and 300 K. If σ_0 takes intermediate values, a gradual transition between Kondo and cotunneling is found. In particular, as shown in Figs. 5(a) and 5(b), for $\sigma_0 \approx 10^{-3}(2e^2)/h$ the predicted gradual transition happens in the same range of temperatures that was experimentally found in the $t = 0.7$ nm junctions. Figure 5(a) shows how

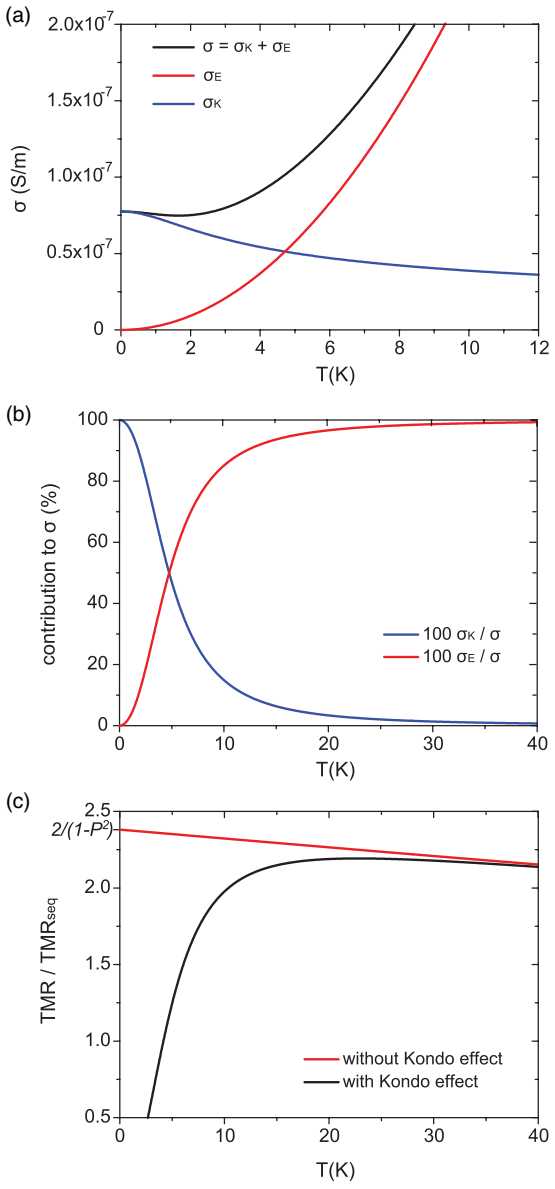

FIG. 5. (Color online) Theoretical model. (a) Total conductivity ($\sigma = \sigma_K + \sigma_E$), elastic conductivity through the clusters without spin flips (σ_E), and conductivity through the clusters showing the Kondo effect (σ_K) vs temperature. (b) Relative contribution to σ of σ_E and σ_K as a function of temperature. (c) Evolution of the TMR with temperature considering and not considering the interplay of the Kondo effect: in the first case σ_K follows Eq. (2), while in the second one $\sigma_K = 0$.

σ approaches σ_K or σ_E as a function of the temperature. The relative contribution of σ_K and σ_E to σ is plotted in Fig. 5(b) for a broader span of temperatures. Note that the selected value of σ_0 is reasonable when we compare with the work of Goldhaber-Gordon *et al.*,[37] who find in their system $\sigma_0 \ll 0.1(2e^2)/h$ if T_K is in the span 10–20 K. We must emphasize that Eq. (2) is only valid for $T \approx T_K$. For clusters of larger volume, T_K rapidly decreases but without any compensating rise in σ_0, leading to an extinction of the Kondo effect. For a discussion of the size of clusters on T_K in a tunneling experiment, see Ref. 39.

B. Tunnel magnetoresistance

The total TMR is due to the contribution of the different conduction channels,

$$\mathrm{TMR} = a\frac{\sigma_D}{\sigma}\mathrm{TMR}_D + b\left(\frac{\sigma_E}{\sigma}\mathrm{TMR}_E + \frac{\sigma_K}{\sigma}\mathrm{TMR}_K\right), \quad (7)$$

where TMR_D is the direct tunneling, TMR_E is the elastic tunneling through the clusters, and TMR_K is the Kondo effect contribution. σ, a, and b come from Eq. (1).

Let us neglect the direct tunneling that was previously done ($a = 0$ and $b = 1$) and assume a perfect suppression of the TMR when the Kondo effect arises, so that $\mathrm{TMR}_K = 0$. According to Takahashi and Maekawa,[14] the dependence of TMR_E on temperature is due to the gradual change from sequential tunneling to cotunneling, and so the TMR is enhanced as T decreases,

$$\mathrm{TMR}_E = \mathrm{TMR}_{\mathrm{cot}}\frac{R_{\mathrm{cot}}}{R_{\mathrm{cot}} + R_{\mathrm{seq}}} + \mathrm{TMR}_{\mathrm{seq}}\frac{R_{\mathrm{seq}}}{R_{\mathrm{cot}} + R_{\mathrm{seq}}}, \quad (8)$$

where $R_{\mathrm{cot}} = \sigma_{\mathrm{cot}}^{-1}$ and $R_{\mathrm{seq}} = \sigma_{\mathrm{seq}}^{-1}$. $\mathrm{TMR}_{\mathrm{cot}}$ and $\mathrm{TMR}_{\mathrm{seq}}$ are the TMR in the cotunneling and sequential tunneling regimes, respectively. Following the same authors,[3,14]

$$\mathrm{TMR}_{\mathrm{cot}} = \frac{2}{1 - P^2}\mathrm{TMR}_{\mathrm{seq}}, \quad (9)$$

where P is the polarization of the electrodes. We can assume $P \approx 0.4$ for our FeCo electrodes, just as for Fe electrodes.[14]

The evaluation of the TMR can be done by normalizing Eq. (7) by $\mathrm{TMR}_{\mathrm{seq}}$. We will use the same values for the different parameters as in Sec. III A, where the gradual transition from cotunneling to the Kondo effect is shown in the conductivity. Figure 5(c) shows the evolution of the TMR with temperature. When decreasing T, the TMR is enhanced a factor $2/(1 - P^2)$ from its value at high temperature ($\mathrm{TMR}/\mathrm{TMR}_{\mathrm{seq}} \approx 1$) due to cotunneling effects. When further decreasing T, the TMR is gradually suppressed due to the Kondo effect. In the figure, we also plot the TMR assuming that there is no Kondo effect, i.e., $\sigma_K = 0$, which helps us to fully appreciate how the suppression due to the Kondo effect takes place. The predicted gradual transition of the TMR happens in roughly the same range of temperatures that was found experimentally in the $t = 0.7$ nm junctions [compare Figs. 5(c) and 4(c)].

The model predicts the existence of a gradual transition even for a monodisperse cluster size distribution. The temperature window for the gradual transition given by the model could be even larger than that shown in Fig. 5 if we were to consider $\sigma_0 > 10^{-3}(2e^2)/h$. Obviously there is some dispersion on the size of the clusters, as shown in the inset of Fig. 1(b), which will lead to a spread in the temperatures at which the crossover from cotunneling to Kondo will happen. However, the dispersion of the size of the clusters cannot explain the differences between the experimental results in DMTJs with CoPt clusters and CoFe since this is similar in both cases.[10] Thus, even if the size dispersion plays its role, we think the experimental behavior of the CoPt-based and CoFe-based junctions can be mainly explained within the framework of this theoretical model. The experimental differences between both types of junctions can be explained considering, for the same size of the clusters, different values of the Kondo contribution (σ_0 or T_K). Note that in this simple theoretical model, the magnetic anisotropy

of the clusters is not taken into account and it can lead to a change in these parameters.[39]

IV. CONCLUSION

The transition between Kondo suppression and cotunneling enhancement of the TMR effects in DMTJs has been studied as a function of the nominal thickness of the discontinuous CoPt layer embedded in an AlO_x barrier and the temperature. Previous work based on CoFe clusters found samples that displayed either one effect or the other.[10] However, in our $Co_{75}Pt_{25}$-based DMTJs, both effects have been found to coexist even in the same sample, for $t = 0.7$ nm, and we are able to tune between them by changing the temperature, as can be seen from the data in Fig. 3(e). The transition temperature was far below the superparamagnetic blocking temperature of the CoPt. This means that (i) there is competition between the different conductance regimes, and their effects in the TMR change gradually with the nominal thickness of the discontinuous layer and the temperature; (ii) the transition is not correlated with the suppression of the fluctuations of the magnetic moment in the clusters as previously thought;[10] and (iii) we made a direct observation of the coexistence of a ferromagnetic phase and the Kondo effect.[16]

In addition, another gradual transition between the Kondo suppression of the TMR and the TMR of the direct tunneling between electrodes was found as the nominal cluster layer thickness was made extremely small. This shows that the spin-flip-related reduction of the TMR in dusted tunnel junctions is due to the contribution of the Kondo effect. Again, during this transition the clusters were stable ferromagnets for all thicknesses at the low temperatures at which we measured.

Finally, we show that the rich behavior of the discontinuous high magnetic anisotropy DMTJs can be understood within the frame of Appelbaum's perturbation theory of conductance.[34,35] Three different contributions to the total conductance are considered: direct tunneling, elastic conductance through the clusters without spin flips, and conductance through the clusters exhibiting the Kondo effect, i.e., spin flips. The model accounts well for the coexistence of the TMR enhancement and suppression in the same sample as a function of the temperature even if no dispersion of the size of the clusters is considered.

The main difference between CoFe and CoPt clusters is the larger spin-orbit coupling in the latter. As a result, there is a higher coercivity in the CoPt clusters which affects the magnetic switching. It also means that the spin is not a good quantum number when the electron is in the CoPt dot. However, the Kondo physics survives this perturbation. The role of the magnetic anisotropy in the Kondo effect is quite complex. Large spin anisotropy usually markedly decreases T_K, inhibiting the Kondo effect. However, for small grains with *planar* anisotropy, which is the case for both the CoPt and CoFe clusters, the magnetic anisotropy can lead to an effective stronger anisotropic Kondo coupling.[39] The experimental differences between CoFe and CoPt clusters suggest that the higher magnetic anisotropy of the CoPt clusters helps to fulfill the theoretical assumptions of the model.

ACKNOWLEDGMENTS

We would like to thank J. S. Moodera, S. Langridge, and C. S. Allen for assistance with the dynamic conductance, SQUID, and STM measurements, respectively. We acknowledge support from the UK EPSRC and the Royal Society, and the State Key Project of Fundamental Research of Ministry of Science and Technology [MOST, No. 2010CB934400], National Natural Science Foundation of China [NSFC, Grants No. 10934099, No. 10874225, and No. 51021061], and K. C. Wong Education Foundation, Hong Kong. Use of the National Synchrotron Light Source, Brookhaven National Laboratory, was supported by the US Department of Energy, Office of Science, Office of Basic Energy Sciences, under Contract No. DE-AC02-98CH10886. D.C. acknowledges support from the Spanish Ministry of Science and Innovation through postdoctoral Grant No. 2008-0352, and a Marie Curie International Outgoing Fellowship within the European 7th Framework Programme.

*dciudad@mit.edu
†Present address: National Institute for Materials Science (NIMS), 1-2-1 Sengen, Tsukuba-city, Ibaraki 305-0047, Japan.
‡Present address: Department of Physics, Durham University, South Road, Durham DH1 3LE, United Kingdom.
§c.h.marrows@leeds.ac.uk

[1] I. Žutić, J. Fabian, and S. Das Sarma, Rev. Mod. Phys. **76**, 323 (2004).
[2] P. Seneor, A. Bernand-Mantel, and F. Petroff, J. Phys.: Condens. Matter **19**, 165222 (2007).
[3] K. J. Dempsey, D. Ciudad, and C. H. Marrows, Philos. Trans. R. Soc. London, Ser. A **369**, 3150 (2011).
[4] A. Bernand-Mantel, P. Seneor, N. Lidgi, M. Muñoz, V. Cros, S. Fusil, K. Bouzehouane, C. Deranlot, A. Vaures, F. Petroff, and A. Fert, Appl. Phys. Lett. **89**, 062502 (2006).
[5] H. Sukegawa, S. Nakamura, A. Hirohata, N. Tezuka, and K. Inomata, Phys. Rev. Lett. **94**, 068304 (2005).
[6] K. J. Dempsey, A. T. Hindmarch, H.-X. Wei, Q.-H. Qin, Z.-C. Wen, W.-X. Wang, G. Vallejo-Fernandez, D. A. Arena, X.-F. Han, and C. H. Marrows, Phys. Rev. B **82**, 214415 (2010).
[7] X.-G. Zhang, Z. C. Wen, H. X. Wei, and X. F. Han, Phys. Rev. B **81**, 155122 (2010).
[8] R. Liu, S.-H. Yang, X. Jiang, T. Topuria, P. M. Rice, C. Rettner, and S. Parkin, Appl. Phys. Lett. **100**, 012401 (2012).
[9] K. Yakushiji, F. Ernult, H. Imamura, K. Yamane, S. Mitani, K. Takanashi, S. Takahashi, S. Maekawa, and H. Fujimori, Nat. Mater. **4**, 57 (2005).
[10] H. Yang, S.-H. Yang, and S. S. P. Parkin, Nano Lett. **8**, 340 (2008).
[11] P. N. Hai, S. Ohya, M. Tanaka, S. E. Barnes, and S. Maekawa, Nature (London) **458**, 489 (2009).
[12] A. Bernand-Mantel, P. Seneor, K. Bouzehouane, S. Fusil, C. Deranlot, F. Petroff, and A. Fert, Nat. Phys. **5**, 920 (2009).
[13] D. V. Averin and Y. V. Nazarov, in *Single Charge Tunneling: Coulomb Blockade Phenomena in Nanostructures*, Vol. 294 of

NATO ASI Series B: Physics, edited by H. Grabert and M. H. Devoret (Plenum, New York, 1992), Chap. 6.
[14]S. Takahashi and S. Maekawa, Phys. Rev. Lett. **80**, 1758 (1998).
[15]J. Martinek, J. Barnaś, A. Fert, S. Maekawa, and G. Schön, J. Appl. Phys. **93**, 8265 (2003).
[16]H. Yang, S.-H. Yang, G. Ilnicki, J. Martinek, and S. S. P. Parkin, Phys. Rev. B **83**, 174437 (2011).
[17]H. X. Wei, Q. H. Qin, M. Ma, R. Sharif, and X. F. Han, J. Appl. Phys. **101**, 09B501 (2007).
[18]L. F. Schelp, A. Fert, F. Fettar, P. Holody, S. F. Lee, J. L. Maurice, F. Petroff, and A. Vaurès, Phys. Rev. B **56**, 5747 (1997).
[19]F. Luis, F. Bartolomé, F. Petroff, J. Bartolomé, L. M. García, C. Deranlot, H. Jaffrès, M. J. Martínez, P. Bencok, F. Wilhelm, A. Rogalev, and N. B. Brookes, Europhys. Lett. **76**, 142 (2006).
[20][http://beamlines.ps.bnl.gov/beamline.aspx?blid=U4B].
[21]A. T. Hindmarch, C. J. Kinane, M. MacKenzie, J. N. Chapman, M. Henini, D. Taylor, D. A. Arena, J. Dvorak, B. J. Hickey, and C. H. Marrows, Phys. Rev. Lett. **100**, 117201 (2008).
[22]A. T. Hindmarch, K. J. Dempsey, D. Ciudad, E. Negusse, D. A. Arena, and C. H. Marrows, Appl. Phys. Lett. **96**, 092501 (2010).
[23]M. F. Hansen and S. Mørup, J. Magn. Magn. Mater. **203**, 214 (1999).
[24]J. M. D. Coey, *Magnetism and Magnetic Materials* (Cambridge University Press, New York, 2010).
[25]J. G. Simmons, J. Appl. Phys. **34**, 1793 (1963).
[26]F. Fettar, S.-F. Lee, F. Petroff, A. Vaurès, P. Holody, L. F. Schelp, and A. Fert, Phys. Rev. B **65**, 174415 (2002).
[27]D. Goldhaber-Gordon, H. Shtrikman, D. Mahalu, D. Abusch-Magder, U. Meirav, and M. A. Kastner, Nature (London) **391**, 156 (1998). S. M. Cronenwett, T. H. Oosterkamp, and L. P. Kouwenhoven, Science **281**, 540 (1998).
[28]H. Yang, Ph.D. thesis, Stanford University, 2006.
[29]C. Romeike, M. R. Wegewijs, W. Hofstetter, and H. Schoeller, Phys. Rev. Lett. **96**, 196601 (2006).
[30]C. Romeike, M. R. Wegewijs, W. Hofstetter, and H. Schoeller, Phys. Rev. Lett. **106**, 019902(E) (2011).
[31]R. Jansen and J. S. Moodera, Phys. Rev. B **61**, 9047 (2000).
[32]R. Guerrero, F. G. Aliev, R. Villar, T. Santos, J. Moodera, V. K. Dugaev, and J. Barnaś, Phys. Rev. B **81**, 014404 (2010).
[33]R. Jansen and J. S. Moodera, J. Appl. Phys. **83**, 6682 (1998).
[34]J. Appelbaum, Phys. Rev. Lett. **17**, 91 (1966).
[35]J. A. Appelbaum, Phys. Rev. **154**, 633 (1967).
[36]P. W. Anderson, Phys. Rev. Lett. **17**, 95 (1966).
[37]D. Goldhaber-Gordon, J. Göres, M. A. Kastner, H. Shtrikman, D. Mahalu, and U. Meirav, Phys. Rev. Lett. **81**, 5225 (1998).
[38]S. T. Ruggiero and J. B. Barner, Z. Phys. B **85**, 333 (1991).
[39]G. A. Fiete, G. Zarand, B. I. Halperin, and Y. Oreg, Phys. Rev. B **66**, 024431 (2002).